Available online at www.sciencedirect.com

ScienceDirect

Procedia Manufacturing 47 (2020) 118–125

Procedia MANUFACTURING

www.elsevier.com/locate/procedia

23rd International Conference on Material Forming (ESAFORM 2020)

On the Applicability of Thermoforming Characterization and Simulation Approaches to Glass Mat Thermoplastic Composites

Dominik Dörr[a,b], Ryan Gergely[c], Stanislav Ivanov[d], Luise Kärger[a], Frank Henning[a,d,e], Andrew Hrymak[d,*]

[a]*Karlsruhe Institute of Technology (KIT), Institute of Vehicle System Technology (FAST), Karlsruhe, Germany.*
[b]*SIMUTENCE GmbH, Karlsruhe, Germany.*
[c]*GM Research and Development, General Motors, Warren, MI, USA.*
[d]*University of Western Ontario (UWO), Faculty of Engineering, London, Ontario, Canada.*
[e]*Fraunhofer Institute for Chemical Technology, Department for Polymer Engineering, Pfinztal, Germany*

** Corresponding author. Tel.: +1 519.661.3110; E-mail address: ahrymak@uwo.ca*

Abstract

Chopped fiber composite materials offer the potential to be used for complex geometries, including local thickness changes, ribs and beads, offering significant potential for functional lightweighting. Depending on the initial mold coverage and flowability of the material, the processing behaves either more like a compression molding or a thermoforming process. The latter is applicable to high initial mold coverages and includes typical thermoforming defects such as local wrinkling. Such defects are not predictable by conventional compression molding simulation approaches usually adopted for this material class. Therefore, thermoforming characterization and simulation approaches and their applicability to glass mat thermoplastic (47 vol.% long glass fiber, Tepex Flowcore) for high initial mold coverages is investigated. Abaqus in combination with several user-subroutines is applied. Valid material characterization results from torsion bar and rheometer bending tests are obtained and applied to an automotive structure in thermoforming simulation. Results indicate that the high stiffness and high viscosity captured by the rheometer bending test at low shear-rates are necessary to reproduce the wrinkling behavior observed in the experimental results. Discrepancy is most likely reducible to thermomechanical effects, and that the modelling approach does not account for thickness deformation due to transverse compression.

Keywords: Chopped fiber materials; glass mat thermoplastics; process simulation; composites; finite element analysis; viscoelasticity; Abaqus

1. Introduction

Lightweighting is an important enabler in the modern automotive industry to reduce greenhouse gas emissions and meet future regulations [1]. For this purpose, continuously fiber-reinforced composites offer a great potential due to their excellent mechanical properties and low density. However, their capability to be shaped into complex geometries is limited. In contrast, chopped fiber materials reveal the potential to be used for more complex geometries, including local thickness changes, ribs and beads, offering a significant potential for functional lightweighting [2,3].

With an eye towards the developments within Industry 4.0, a continuous and functional virtual process chain is a powerful tool. Thereby, a digital twin of the production process by means of process simulation is suitable for optimization of manufacturing processes. In the context of a continuous virtual process chain, it enables the robust development and virtual testing of new components or the adjustment of components to changes in boundary conditions [2].

10.1016/j.promfg.2020.04.148

The material investigated within this study is Tepex Flowcore, a long glass fiber reinforced polyamide (PA/GF) glass mat manufactured by Lanxess, Bond Laminates. This material can be characterized by high fiber volume content (47 vol.%), random fiber orientation and consistent fiber length distribution. Tepex Flowcore consists of long (30-50mm) glass fibers with an engineering polymer, i.e. PA6, and belongs to the material class of Glass Mat Thermoplastic (GMT). Depending on the initial mold coverage and flowability of the material, processing behaves more like either a compression molding or a thermoforming process. When initial mold coverage is low, the processing is more like compression molding, where the material is required to flow to fill the mold. When the initial mold coverage is high, the processing is more like thermoforming, where there is little or no flow of material, and includes typical thermoforming defects such as local wrinkling. Therefore, it becomes of utmost interest to predict both compression molding and thermoforming processing behavior, and to evaluate the limits of each simulation approach.

Regarding compression molding simulation, approaches have been developed that apply two-phase methods based on Darcy's law [4] or separate fiber and matrix speeds with a model transition for different flow regimes [5]. Direct fiber simulations [6] are another two-phase method that enable detailed studies on fiber orientation, e.g. at rib geometries [7]. However, the majority of these approaches consider the material during compression molding as a single phase using Eulerian or Arbitrary Lagrangian Eulerian (ALE) models. In recent publications [2,8,9], Sheet Molding Compound (SMC), also a chopped fiber material but with a thermoset matrix, is modelled as a three dimensional, one-phase, weakly compressible, anisotropic, non-Newtonian material that experiences slip at the mold surface due to a lubrication layer. A similar approach is conceivable for GMT materials, since these approaches are in general capable of modeling flow behavior of highly concentrated fiber suspensions.

However, typical thermoforming defects such as wrinkling behavior are not predictable by compression molding simulation approaches, since these are meant to predict flow behavior. In contrast, thermoforming simulation explicitly aims to predict such defects for continuously fiber-reinforced thermoplastic tape laminates [10,11,12], using purely Lagrangian modeling approaches. In this context, most of these approaches utilize conventional shell elements, due to the high slenderness ratio of the according pre-products. Only few studies consider three-dimensional approaches thus far, since often these materials reveal a specific behavior under bending loading, which cannot directly be captured by first order material modeling approaches [13].

In this study, characterization and modeling techniques originating from thermoforming simulation are applied to Tepex Flowcore, in order to investigate their suitability for the thermoforming-like processing behavior for high mold coverages. Thereby, this study is delimited to isothermal and conventional shell element analyses, targeting a modeling approach with the least possible complexity.

2. Material characterization

For intra-ply material characterization of thermoplastic UD-tape laminates for thermoforming simulation, usually the torsion bar test presented by Haanappel et al. [14] and the rheometer bending test presented by Sachs et al. [15] are applied. Based on this, membrane and bending behavior are characterized, respectively, due to the requirement for modeling these deformation mechanisms in a decoupled fashion, since conventional plate theories are not applicable for thermoforming simulation [10-12,16]. Both tests are conducted on the Tepex Flowcore material at Fraunhofer ICT in Pfinztal, Germany on an Anton Paar MCR 501 rheometer equipped with a thermal chamber CTD 450, which is nitrogen-purged to avoid thermo-oxidative degradation of the polymer.

(a) (b)

Fig. 1: Thermoforming characterization setups applied to Tepex Flowcore: a) Torsion bar test and b) rheometer bending test.

2.1. Torsion bar test

The torsion bar characterization setup (cf. Figure 1a) deals with a prismatic bar, which is subjected to torsion and the resulting torsional moment is captured as the characterization result. Usually, the fibers of the tested UD-tape laminates are aligned along the long axis of the specimen. However, no principal material orientation exists for Tepex Flowcore, since the fibers are randomly oriented. The tested specimens measure 60.0 x 13.0 x 10.4 mm³ and consist of 10 pre-consolidated layers. An isothermal and transient testing procedure is applied, where the specimens are deflected to 60° under variation of deformation rate (0.1, 1.0, 10.0 rpm) and temperature (230, 250, 270 °C) according to a full factorial testing plan. Three replicates are conducted for the intermediate temperature and a single replicate for the remaining design points.

Figure 2 shows an excerpt of the characterization results. The initial overshoot of the measured moment for the high deformation rate at low deflection angles is attributed to inertia effects and the control system of the rheometer (10.0 rpm, Figure 2a). The moment-deflection-curves reveal a distinct rate-dependency for each temperature, which is exemplified for the intermediate temperature of 250 °C. Furthermore, a distinct temperature-dependency is observed, as exemplified for the intermediate deformation rate of 1.0 rpm (Figure 2b). The characterization results show, in general, the same characteristic behavior as is also observed for thermoplastic UD-tape laminates with the same polymer, but with a different magnitude of torsion moment [10,11].

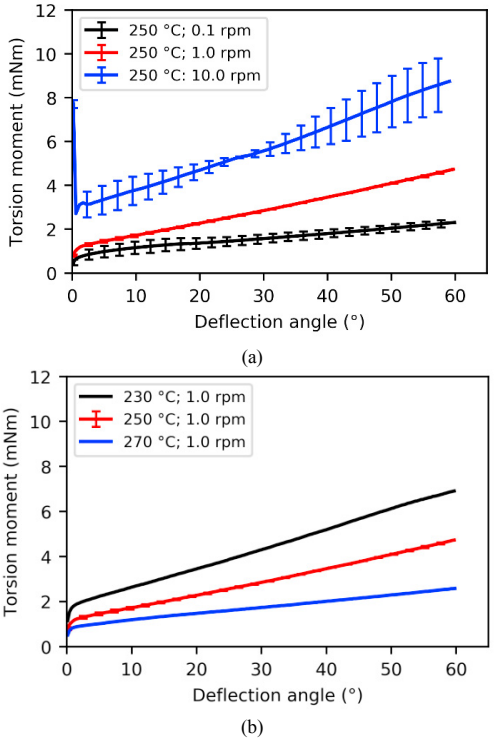

Fig. 2: Excerpt of the torsion bar test results obtained for Tepex Flowcore. a) Three deformation rates at the same temperature (250 °C). b) Three temperatures at the same deformation rate (1.0 rpm). Error bars represent one standard deviation (n = 3).

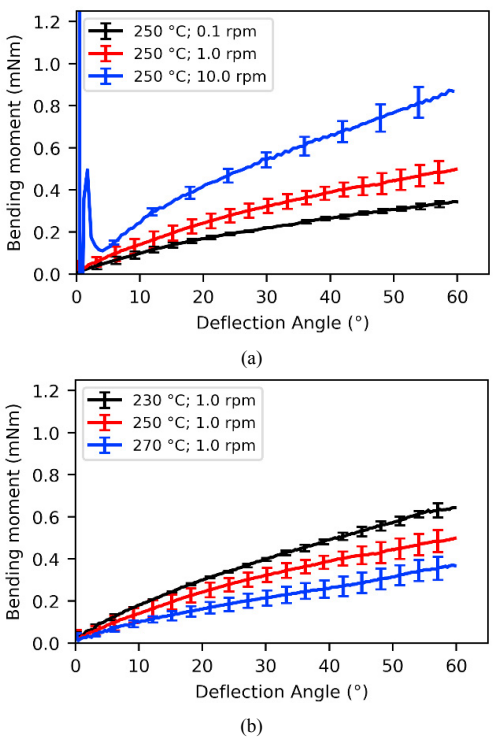

Fig. 3: Excerpt of the bending test results obtained for Tepex Flowcore. a) Three deformation rates at the same temperature (250 °C). b) Three temperatures at the same deformation rate (1.0 rpm). Error bars represent one standard deviation (n = 3).

2.2. Rheometer bending test

The rheometer bending test utilizes a custom bending setup (cf. Figure 1b), which transforms the rotation of the upper rheometer shaft to a bending load. The tested specimens are single plies of Tepex Flowcore with 1.0 mm thickness, measure 35.0 x 25.0 mm², and are covered with polyimide tape at both ends, to guarantee free sliding within the fixture. An isothermal and transient testing procedure is applied, where the specimens are deflected to 60° under variation of deformation rate (0.1, 1.0, 10.0 rpm) and temperature (230, 250, 270 °C) according to a full factorial testing plan. Three replicates are conducted for all design points.

Figure 3 shows an excerpt of the obtained characterization results. The same characteristics as for the torsion bar test are observed. Again, the initial overshot of the measured moment for the high deformation rate at low deflection angles is attributed to inertia effects and to the control system of the rheometer (10.0 rpm, Figure 3a). The moment-deflection-curves reveal a distinct rate-dependency for each of the investigated temperatures, which is exemplified for the intermediate temperature of 250 °C. Furthermore, a distinct increase of material stiffness is observed for decreasing temperatures, as exemplified for the intermediate deformation of 1.0 rpm (Figure 3b). In analogy to the torsion bar tests, the characterization results show, in general, the same characteristic behavior as also observed for thermoplastic UD-tape laminates with the same polymer, but with a different magnitude of bending moment [10,11].

3. Material modeling and parameterization

The characterization results presented in Section 2 are employed for parametrization of the material model for thermoforming simulation. For this purpose, the characterization tests are modeled using Finite Element Analysis (FEA) (cf. Figure 4) and material parameters are identified inversely by a gradient-based optimization procedure, used to fit the moment-deflection-curves obtained from FEA to the characterization test data.

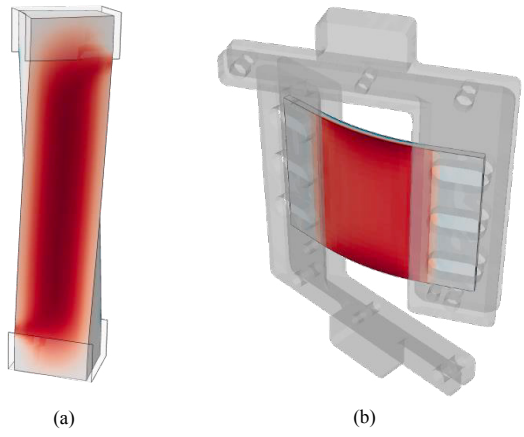

Fig. 4: FEA models for the characterization setups: a) Torsion bar test (shear strain). b) Rheometer bending test (bending strain).

3.1. Membrane behavior

Membrane behavior is modeled by a nonlinear Voigt-Kelvin approach with an isotropic stiffness and a shear-rate-dependent viscosity [10,11], where the total Cauchy stress is given by

$$\boldsymbol{\sigma} = \boldsymbol{\sigma}^{\mathrm{el}} + \boldsymbol{\sigma}^{\mathrm{visc}}. \tag{1}$$

Here, $\boldsymbol{\sigma}^{\mathrm{el}}$ is the elastic and $\boldsymbol{\sigma}^{\mathrm{visc}}$ the viscous part. The elastic part is modeled by a St. Venant-Kirchhoff material defined by

$$\boldsymbol{S}^{\mathrm{el}} = \mathbb{C}\colon \boldsymbol{E} \quad \text{with} \quad \boldsymbol{\sigma}^{\mathrm{el}} = J^{-1}\boldsymbol{F}\cdot\boldsymbol{S}^{\mathrm{el}}\cdot\boldsymbol{F}^{\mathrm{T}} \quad \text{and} \quad J = \det(\boldsymbol{F}), \tag{2}$$

where $\boldsymbol{S}^{\mathrm{el}}$ is the second Piola-Kirchoff stress, $\mathbb{C}$ the fourth-order elastic stiffness tensor, $\boldsymbol{E}$ the Green-Lagrange strain and $\boldsymbol{F}$ the deformation gradient. The viscous part is modeled by a Cross model:

$$\boldsymbol{\sigma}^{\mathrm{visc}} = J^{-1}2\eta\boldsymbol{D} \quad \text{with} \quad \eta = \frac{\eta_0-\eta_\infty}{1-m\dot{\gamma}^{1-n}} + \eta_\infty, \tag{3}$$

where $\boldsymbol{D}$ is the rate-of-deformation tensor, η the viscosity, $\dot{\gamma}$ the shear-rate and η_0, η_∞, m and n are material properties. These equations are implemented in Abaqus as a user-material subroutine (UMAT), where the isotropic elastic stiffness $\mathbb{C}$ and the viscosity η are determined by the above outlined parameterization procedure. In the related FEA, the rigid body fixture of the torsion bar test is modelled by rigid surfaces and the specimen is modelled by hybrid, linear and three-dimensional brick elements (C3D8H) (cf. Figure 4a). This element type has three translational degrees of freedom at each node and one additional pressure degree of freedom, which is adopted to invoke material incompressibility. Full integration is applied, to prevent the necessity to use hourglass stabilization.

Figure 5 shows exemplary parameterization results at 250 °C, revealing that the nonlinear Voigt-Kelvin approach yields a constant slope for each deformation rate, which is induced by the elastic stiffness, and a constant offset between the curves, which is induced by the nonlinear viscosity model. A good agreement is observed for the intermediate and low deformation rate. In contrast, deviations are observed for the high deformation rate, since the slopes of the moment deflection curves increase with increasing deformation rate. The same characteristic is also observed for thermoplastic UD-tape laminates with the same polymer [10,11]. It was previously shown that this deviation has a minor influence in thermoforming simulation [10].

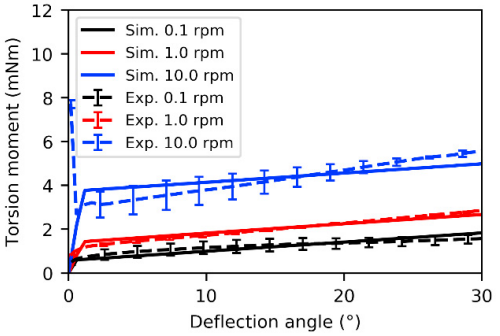

Fig. 5: Parameterization results according to the torsion bar test for membrane modeling at 250 °C.

3.2. Bending behavior

Bending behavior is modeled, in analogy to membrane behavior, using a nonlinear Voigt-Kelvin approach with an isotropic stiffness and a shear-rate-dependent viscosity. Therefore, Equation 1 applies also here. In contrast to membrane behavior, a hypoelastic approach in combination with a fiber-parallel material frame is adopted here to model the elastic part $\boldsymbol{\sigma}^{\mathrm{el}}$ by [10,16]

$$[\boldsymbol{\sigma}^{\nabla}]_{\{\boldsymbol{g}_i^*\otimes\boldsymbol{g}_j^*\}} = [\mathbb{C}]_{\{\boldsymbol{g}_i^*\otimes\boldsymbol{g}_j^*\otimes\boldsymbol{g}_k^*\otimes\boldsymbol{g}_l^*\}}\colon[\boldsymbol{D}]_{\{\boldsymbol{g}^{*k}\otimes\boldsymbol{g}^{*l}\}}, \tag{4}$$

due to the restrictions within the adopted user-interface of Abaqus for shell section integration ((V)UGENS). Here, $\boldsymbol{D}$ is the rate-of-deformation tensor and $\boldsymbol{g}_i^*$ and $\boldsymbol{g}^{*i}$ are the co- and contravariant principal material directions of the fiber-parallel frame, respectively. For the viscous part $\boldsymbol{\sigma}^{\mathrm{visc}}$, Equation 3 applies also for bending behavior.

For parameter identification by means of FEA, the bending setup is modelled as a rigid surface and the specimen is modelled by means of superimposed membrane (M3D4) and shell elements (S4R) (cf. Figure 4b). The user-interface for shell section integration (UGENS) is assigned to the shell elements, in order to neglect the membrane part of the shell element, yielding a fully decoupled membrane and bending behavior [10,16], which is a basic requirement on thermoforming simulation using conventional shell elements.

Figure 6 shows exemplary parameterization results at 250 °C, revealing a similar characteristic as also observed for membrane behavior. Thus, the nonlinear Voigt-Kelvin approach yields a constant slope for each deformation rate, which is induced by the elastic stiffness, and a constant offset between the curves, which is induced by the nonlinear viscosity model. A good agreement is observed for the intermediate and low deformation rate. In contrast, deviations are observed for the high deformation rate, since the slopes of the moment deflection curves increase with increasing deformation rate. The same characteristic is also observed for thermoplastic UD-tape laminates with the same polymer [10,16]. Besides this, some minor oscillations are observed for the high deformation rate in FEA, which is attributed to the nonlinear nature of the viscosity model and the instantaneous change of shear-rate at the onset of deformation.

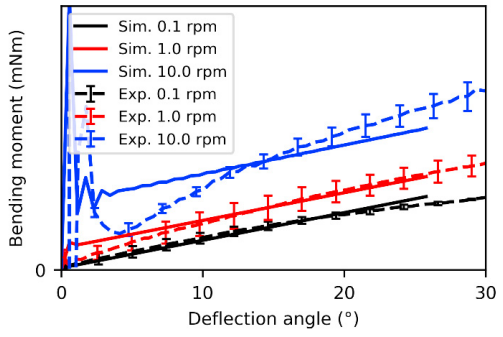

Fig. 6: Parameterization results according to the rheometer bending tests for bending modeling at 250 °C.

3.3. Comparison of membrane and bending behavior

The preceding parameterization approach based on the two different characterization methods originates from highly anisotropic UD-tape materials with extremely low bending stiffness compared to membrane stiffness in fiber direction. The approach essentially yields two separate material models for membrane and bending behavior for the same material at a given temperature. These two material models are then combined in a decoupled modeling of membrane and bending to represent the material. Since the fiber architecture of Tepex Flowcore with randomly oriented fibers is completely different to that of unidirectional fiber-reinforced thermoplastic tapes, it is questionable if the membrane-bending-decoupling is necessary. Therefore, a single isotropic material model, without decoupling between membrane and bending behavior, is sought for this material including a constant elastic stiffness $\mathbb{C}$ and a constant Cross model viscosity η. In order to compare the results for the two test methods and three deformation rates, $\mathbb{C}$ and η are determined for each design point of the torsion bar (TB) and rheometer bending (RB) tests.

Figure 7 shows the results for the isotropic elasticity modulus E (Figure 7a) used to determine the elastic stiffness $\mathbb{C}$ and the isotropic viscosity η (Figure 7b).

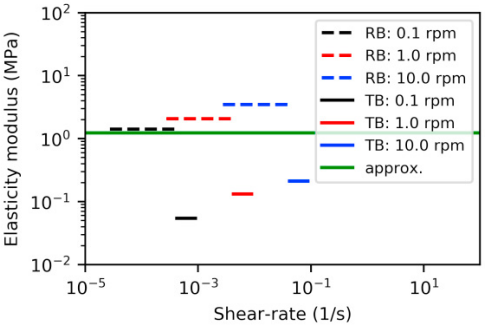

(a)

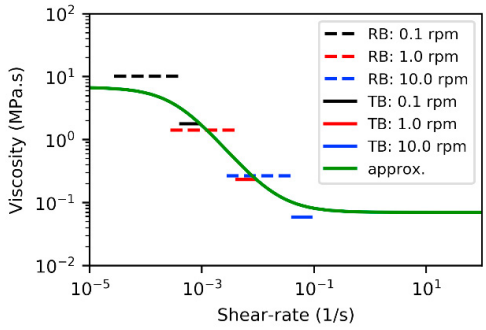

(b)

Fig. 7: Parameterization results for the torsion bar (TB) and rheometer bending (RB) tests as well as approximated average for a) constant isotropic elasticity modulus E and b) constant isotropic viscosity η and w.r.t. to shear-rate $\dot{\gamma}$ at 250 C.

These values are plotted with respect to 25 - 75 % of the shear-rates observed in the related FEA for each of the tests at 250 °C for the three different deformation rates. Regarding the elasticity modulus (cf. Figure 7a), very low values and an increase for higher shear-rates are observed for both tests. Here, the observed values differ by one order of magnitude between the rheometer bending and torsion bar tests. However, since the elasticity moduli are very low, it is questionable if there is a sensitivity of the deformation behavior to the elastic part of the Voigt-Kelvin approach during thermoforming simulation. The average (arithmetic mean) elasticity modulus for all six tests is shown as a green horizontal line.

For viscosity (cf. Figure 7b), shear-thinning behavior is observed, which is a well-known phenomenon for polymer liquids [17]. An overlapping of shear-rates from the two different tests, with good agreement of the obtained viscosity values, is observed. Therefore, the results from the two test methods can be combined into a single parameterization of a rate-dependent viscosity using the Cross model, represented by the green line.

If the discrepancy between the two tests in the elastic part can be neglected, it can be represented by a single combined parameter set. This would then make the decoupling of membrane and bending behavior unnecessary, since highly comparable viscosity values are determined from the torsion bar and rheometer bending test.

4. Application to thermoforming simulation

For application of the above outlined material modeling and parameterization approaches to Tepex Flowcore in thermoforming simulation, a geometry referred to as a seatback outer is adopted (Figure 8). The seatback outer is a complexly shaped structural part, which is designed to be joined together with a second part, the seatback inner. It has narrow deep draw areas, and various features including beads and local thickness changes.

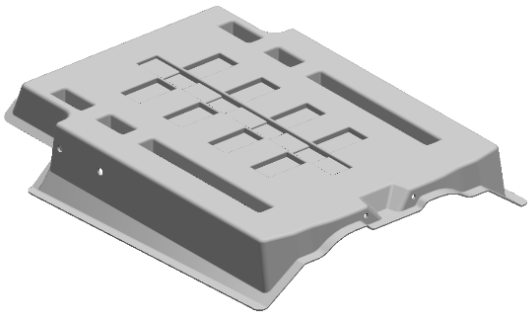

Fig. 8: Geometry of the seatback outer used as application example for thermoforming simulation.

Figure 9 shows the thermoforming simulation setup in Abaqus. The shear edge tooling is modeled as rigid surfaces and related tool kinematics are modeled by a displacement boundary condition in real-time, to accurately account for the rate-dependent material behavior. Thereby, explicit time integration is applied in combination with an appropriate mass scaling for an efficient analysis. The formed blank is a single ply of Tepex Flowcore with 2 mm thickness, which is modeled isothermally using superimposed membrane and conventional

shell elements, where the approaches outlined and parametrized in Section 3 are adopted.

Three different scenarios are considered. First, the usually applied approach for decoupling of membrane and bending behavior is applied. Second, the torsion bar parameter set is applied for modeling both membrane and bending behaviors. Third, the rheometer bending parameter set is applied for modeling both membrane and bending behavior. Thereby, the last two scenarios imply that conventional shell theory is adopted (not decoupled).

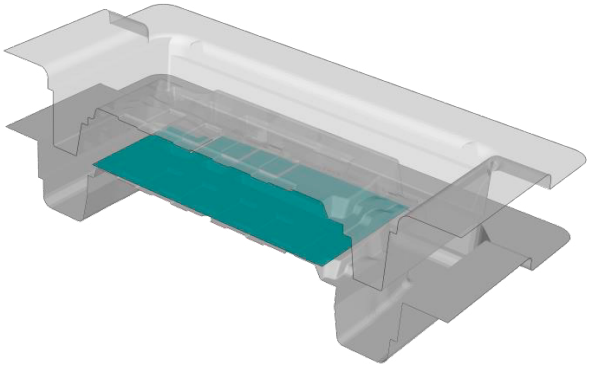

Fig. 9: Abaqus thermoforming simulation setup for the seatback outer geometry in cross-sectional view at the line of symmetry with transparent blank (teal) and upper tool.

4.1. Simulation results

Figure 10 shows the obtained isothermal simulation results at 250 °C for a remaining tool travel of 5 mm. The colormap indicates the transverse Green-Lagrange strain E_{33}, where blue indicates material thinning, and red indicates material thickening. For all scenarios, distinct local thinning due to in-plane elongation and the incompressibility constraint is observed in the areas of the deep drawn features. Thereby, a good formability and no wrinkling behavior is observed for Scenario 1 (cf. Figure 10a). In contrast, slight local wrinkling behavior is observed around the deep drawn sections for Scenario 2 (cf. Figure 10b) and distinct local wrinkling behavior for Scenario 3 (cf. Figure 10c).

In general, wrinkling is an instability issue, which is determined by a balance between membrane and bending stiffness. Therefore, the increasing wrinkling behavior for Scenario 2 is attributed to the decreasing bending stiffness modeled by the TB parameter set compared to the RB parameter set. In contrast, the further increase of wrinkling behavior for Scenario 3 is attributed to the increasing membrane stiffness according to the RB parameter set, since the higher viscosity and elasticity moduli values are adopted (cf. Figure 7).

The presented thermoforming simulation results show a distinct dependency of the choice of parameter sets from torsion bar and rheometer bending testing for membrane and bending modeling. However, both characterization tests could be described by a single parameter set at least on average, as outlined in Section 3.3. Therefore, a fourth scenario is considered, where the viscosity of both characterization tests is approximated by a Cross model and the elasticity modulus by the arithmetic mean (cf. Figure 7).

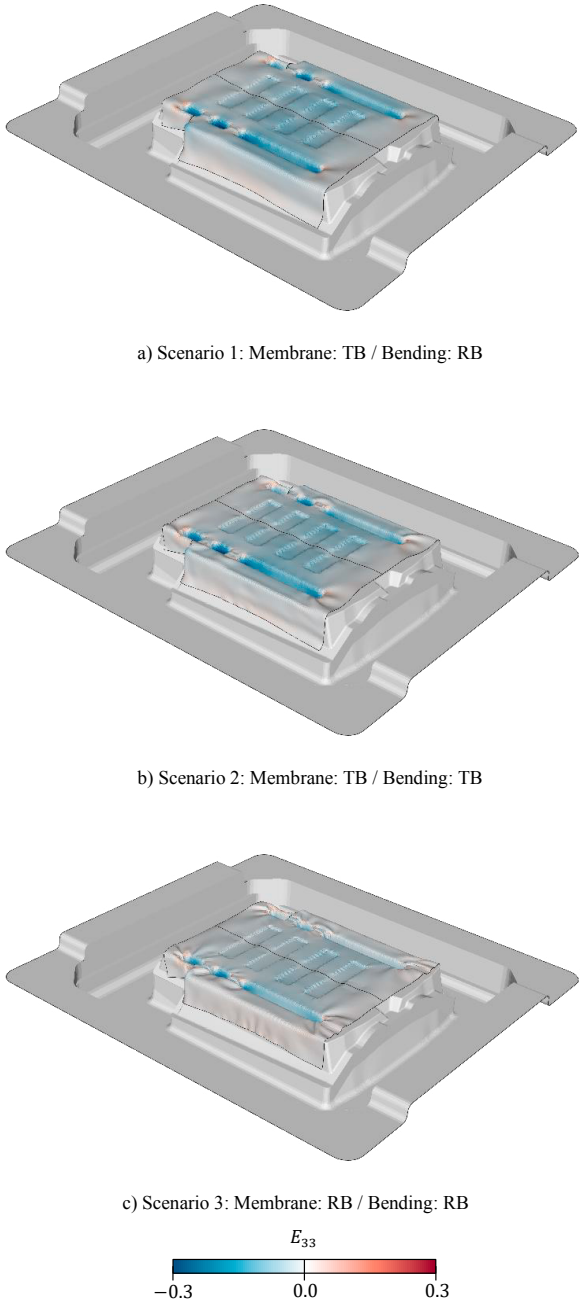

Fig. 10: Thermoforming simulation results for the seatback outer geometry: Transverse Green-Lagrange strain E_{33} under variation of the parameter sets for membrane and bending modeling for a remaining tool travel of 5 mm.

The results of Scenario 4 are shown in Figure 11. A similar amount and direction of wrinkles compared to Scenario 3 is observed. Thus, the rheometer bending parameter set, and the combined single parameter set yield similar predicted formability. Hence, the high stiffness and high viscosity

captured in the rheometer bending tests particularly at low shear-rates has a pronounced effect on the results.

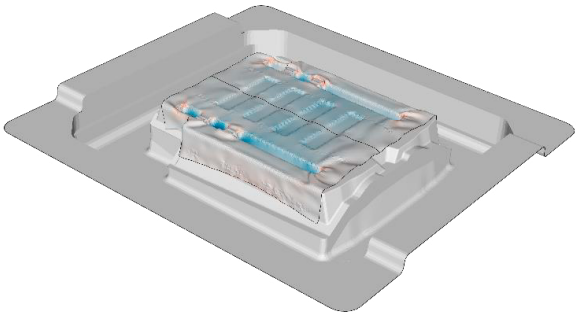

Fig. 11: Thermoforming simulation result for a parameter set approximating both, the torsion bar and rheometer bending test, for a remaining tool travel of 5 mm.

4.2. Experimental thermoforming test

Figure 12 shows a surface measurement of an experimental thermoforming test for the seatback outer geometry at a remaining tool travel of 5 mm.

Fig. 12: Surface scan of the experimental thermoforming result for the seatback outer geometry for a remaining tool travel of 5 mm.

The experimental test shows wrinkling behavior around the deep draw areas, which is in agreement with thermoforming simulation for Scenarios 3 and 4. However, wrinkling is observed in the experimental test additionally for the inner part areas, as well as at the part flanges, which is not predicted by thermoforming simulation.

5. Discussion and conclusion

Thermoforming characterization and simulation approaches are applied to Tepex Flowcore, a Glass Mat Thermoplastic (GMT) with an engineering polymer matrix, i.e. PA6. Torsion bar and rheometer bending testing, which are usually adopted for characterization of membrane and bending behavior of thermoplastic UD-tapes for thermoforming simulation, show reasonable results. Thereby, a distinct temperature- and rate-dependent material behavior is observed.

The presented characterization results are applied for parametrization of material modeling approaches for thermoforming simulation based on a nonlinear Voigt-Kelvin approach. The parameterization results reveal that the Voigt-Kelvin approach is capable to describe the material characteristic in average, where deviations are observed for the high deformation rate. However, previous studies on thermoforming simulation have shown that deviations of this order of magnitude show minor influences in thermoforming simulation [10,16]. In addition, the same viscosity values are determined from the two different tests for the same shear-rate, accompanied with very low values for the elasticity modulus. This brings into question whether the usually adopted decoupling of membrane and bending behavior is necessary for Tepex Flowcore, furthermore for GMT materials, when applying thermoforming simulation.

Finally, the different parameter sets are applied to thermoforming simulation of a complex geometry. The results reveal that wrinkling behavior around the deep draw areas is predicted when applying the parameter set obtained from rheometer bending testing to both membrane and bending modeling, as well as when applying the combined parameter set which describes both characterization tests approximately. Thus, characterization by the rheometer bending test at low shear-rates and related high viscosity and stiffness are relevant and should be considered.

Wrinkling around the deep draw areas is also observed in experimental tests. However, the experimental tests show more pronounced wrinkling behavior. The deviation in the amount of wrinkles might be attributed to thermomechanical effects, as has also been observed for thermoplastic UD-tapes [10,11], which are not considered in the isothermal analyses of this study. In addition, transversal compaction and its impact on material thinning is not considered in this simulation approach thus far.

Therefore, future studies will focus on the implementation of a thermomechanical 3D approach, which is straightforward, since membrane bending decoupling is not strictly necessary. For this purpose, a combination of the thermomechanical thermoforming simulation approach presented by Dörr et al. [10,11] and the equation of state and viscosity models presented by Görthofer et al. [2] will be pursued.

Acknowledgements

The authors acknowledge the funding support of General Motors of Canada, Natural Sciences and Engineering Research Council of Canada (Grant CRDPJ 518279-17) and the Ontario Centres of Excellence (Grant VIP2 28722). Furthermore, the authors gratefully appreciate the carefully carried out characterization tests by Susanne Lüssenheide (Fraunhofer ICT, Pfinztal, Germany).

References

[1] Henning F, Kärger L, Dörr D, Schirmaier FJ, Seuffert J, Bernath A. Fast processing and continuous simulation of automotive structural composite components. Composites Science and Technology 2019(171):261–79.

[2] Görthofer J, Meyer N, Pallicity TD, Schöttl L, Trauth A, Schemmann M et al. Virtual process chain of sheet molding compound: Development, validation and perspectives. Composites Part B: Engineering 2019(169):133–47.

[3] Tatara RA. Compression Molding. Applied Plastics Engineering Handbook, William Andrew, Waltham, USA, 2017, 291–320.

[4] Orgéas L, Idris Z, Geindreau C, Bloch JF, Auriault JL. Modelling the flow of powerlaw fluids through anisotropic porous media at low-pore Reynolds number. Chem Eng Sci Jul. 2006;61(14):4490–502.

[5] Perez-Miguel M, Abisset-Chavanne E, Chinesta F, Keunings R. From dilute to entangled fiber suspensions involved in reinforced polymers and composites. AIP conference proceedings, vol. 1896. 2017:030006.

[6] Fan X, Phan-Thien N, Zheng R. A direct simulation of fibre suspensions. J. Nonnewton. Fluid Mech. Jan. 1998;74(1–3):113–35.

[7] Kuhn C, Walter I, Täger O, Osswald T. Simulative prediction of fiber-matrix separation in rib filling during compression molding using a direct fiber simulation. J. Compos. Sci. Dec. 2017;2(1):2

[8] Guiraud O, Dumont PJJ, Orgéas L, Favier D. Rheometry of compression moulded fibre-reinforced polymer composites: Rheology, compressibility, and friction forces with mould surfaces. Compos. Part A Appl Sci Manuf Nov. 2012;43(11):2107–19.

[9] Hohberg M, Kärger L, Henning F, Hrymak A.: Rheological Measurements and Rheological Shell Model considering the Compressible Behavior of Long Fiber Reinforced Sheet Molding Compound (SMC). Composites Part A 95: 110-117, 2017.

[10] Dörr D. Simulation of the thermoforming process of UD fiber-reinforced thermoplastic tape laminates, Doctoral thesis, Karlsruhe Institute of Technology (KIT), Institute of Vehicle System Technology (FAST), 2019.

[11] Dörr D, Joppich T, Henning, F., Kärger, L. A coupled thermomechanical approach for finite element forming simulation of continuously fiber-reinforced semi-crystalline thermoplastics. Composites Part A: Applied Science and Manufacturing 2019(125):105508.

[12] Haanappel SP, Thije R ten, Sachs U, Rietman B, Akkerman R. Formability analyses of uni-directional and textile reinforced thermoplastics. Composites Part A: Applied Science and Manufacturing 2014;56:80–92.

[13] Boisse P, Bai R, Colmars J, Hamila N, Liang B, Madeo A. The Need to Use Generalized Continuum Mechanics to Model 3D Textile Composite Forming. Appl Compos Mater 2018;47(11):7.

[14] Haanappel SP, Akkerman R. Shear characterisation of uni-directional fibre reinforced thermoplastic melts by means of torsion. Composites Part A: Applied Science and Manufacturing 2014;56:8–26.

[15] Sachs U, Akkerman R. Viscoelastic bending model for continuous fiber-reinforced thermoplastic composites in melt. Composites Part A: Applied Science and Manufacturing(100):333–41.

[16] Dörr D, Schirmaier FJ, Henning F, Kärger L. A viscoelastic approach for modeling bending behavior in finite element forming simulation of continuously fiber reinforced composites. Composites Part A: Applied Science and Manufacturing 2017;94:113–23.

[17] Han C D. Rheology and processing of polymeric materials: Volume 1: Polymer rheology. Oxford University Press, Oxford and New York, 2007.